A comparison of modeling frameworks for the oscillatory silicon electrodissolution

Konrad Schönleber, Maximilian Patzauer, Katharina Krischer*

Non-equilibrium Chemical Physics, Physik-Department, Technische Universität München, 85747 Garching, Germany

Abstract

The emergence of oscillations during the silicon electrodissolution has often been tackled using a framework where the global oscillatory signal is seen as the outcome of a synchronization of self-oscillatory microdomains with a certain frequency distribution. It is the main objective of this publication to reject this widely adopted modeling framework by showing that it is incompatible with spatially resolved experiments. Instead, we propose a fundamentally different modeling framework where the system is seen as an oscillatory medium.

Keywords: silicon electrochemistry, electrochemical oscillations, oscillatory medium, synchronization

1. Introduction

The oscillatory electrodissolution of silicon in fluoride containing media has attracted a lot of interest in the decades since its first finding by Turner in 1958 [1, 2]. Despite the intense research efforts and the wealth of experimental findings both under potentiostatic and galvanostatic control, a mechanism of what causes these oscillations is still missing. Nevertheless, there is an immense amount of speculation on the topic and based on the numerous experimental results many promising candidates for physical quantities participating in the oscillation mechanism such as physical stress or electrical quantities have been put forward [3–5]. Two influential publications from Chazalviel et al. [6, 7] 25 years ago have set a framework for modeling efforts taken up by many groups [8–11]. These publications are concerned with oscillations of the current under potentiostatic control with an external resistance, but the same modeling framework has also been used to explain potential oscillations under galvanostatic control [12]. In this framework the electrode is thought to be composed of oscillatory microdomains with some frequency distribution. These microdomains are believed to be desynchronized in general with a steady global current as the outcome. Only when an external coupling is present, for example imposed by an external resistance, these microdomains oscillate with a high degree of synchrony and thus produce a macroscopic oscillation. In the absence of the external coupling only transient oscillation are observed. These are thought to be brought about by a voltage jump from a value outside of the stable oxide region, typically < 2 V vs. SHE, to the region where oscillations occur, typically > 3.5 V vs. SHE [2], resulting in an initially strong degree of synchronization between the microdomains. This is then gradually lost leading to a non-oscillatory steady state as the long term behavior. This means that, in this view, the local oscillatory behavior is persisting even in the globally non-oscillatory state of the system. Overall the local oscillator modeling framework is strongly reminiscent of the Kuramoto model, where the behavior of globally coupled phase oscillators is treated in a quite general manner [13, 14]. Specifically, the Kuramoto model explains the surprising formation of oscillator groups with approximately identical phases only above a certain threshold value of the global coupling strength.

The local oscillator framework was established as a means to explain a number of experimental findings where three findings were especially addressed. First, stable oscillations are only found above an electrolyte-specific threshold value of the external resistance and transient oscillations are found below this value [15]. Second, impedance spectra recorded in the steady state show resonances at the base frequency of the above-threshold oscillation and its overtones [7]. Third, when the anodization voltage is switched to a value slightly above the open circuit potential of the sample, transient anodic currents have been found [16, 17]. The shape and total charge of these current peaks were then found to be phase dependent in the case of stable oscillations and an averaged value of these phase dependent curves was observed in the corresponding steady state obtained without external resistance [18].

At first glance, the view of a spatially inhomogeneous electrode behavior is tempting, since electrified interfaces are rarely inherently homogeneous due to for example qualitatively different reaction sites such as kink or terrace sites or different crystal facets. However, it has to be noted that often spatially long-range couplings equalize local differences. These global quantities, as for example the average potential drop across the interface, then govern the local behavior and not the other way around [19]. This is well demonstrated for nonlinear behavior at metal electrodes, and in the case of the CO oxidation on platinum electrodes the emergence of bistability or oscillations could be well described with mean field models [20, 21]. In

*Corresponding author
Email address: krischer@tum.de (Katharina Krischer)

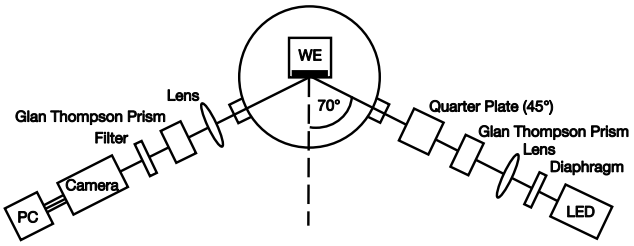

Figure 1: Schematic of the experimental setup used for the in-situ measurements of the spatio-temporal evolution of the oxide layer in silicon electrodissolution experiments.

these cases the interface is best described as a homogeneous medium. We strongly favor this view also for the silicon electrodissolution system.
In the following we will argue that the local oscillator framework does not stand up to further experimental testing, specifically to spatially resolved measurements. Instead we propose to look at the silicon electrodissolution system as a uniform oscillatory medium.

2. Experimental system

Our spatially resolved measurements of the temporal development of the oxide layer thickness $\xi(\vec{x})$ are obtained with an in-situ ellipsometric imaging system as schematically shown in Fig.(1). We use a conventional three electrode setup where great care is taken to assure uniform experimental parameters at the silicon interface, which has an approximately rectangular shape and an area of around 4×5 mm^2. Specifically, the electrolyte (350 ml) is continuously stirred, unless stated otherwise, and the counter electrode is a ring-shaped platinum wire placed symmetrically several cm in front of the working electrode. The reference electrode is placed relatively far away from the other electrodes outside of the current path. The experimental setup and sample preparation is described in detail in earlier publications [22, 23].

3. Results

We focus our attention on the measurement of a series of stable sinusoidal oscillations with an amplitude decreasing with decreasing global coupling strength, mediated by a decreasing value of the external resistance. In the local oscillator view the change in amplitude corresponds to a change in the degree of synchronization while the local oscillators are mostly unaffected. Conversely, in the framework of an oscillatory medium the same series of resistances corresponds to a gradual shift in a parameter governing both the local oscillatory dynamics and the coupling of the points at the surface. The change between the oscillatory and non-oscillatory state occurs here via a Hopf bifurcation at a critical lower value of the external resistance. The series of measurements presented below has been

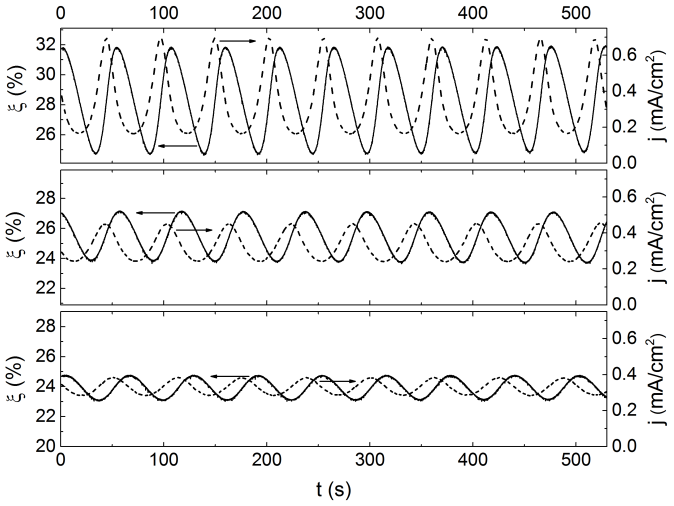

Figure 2: Time series of ξ (solid lines left scale) and j (dashed lines right scale) for oscillations with a constant $\overline{U_{\rm el}} = 8$ V vs. SHE in an electrolyte with $c_{\rm F} = 60$ mM, pH $= 1$ for $R_{\rm ext}A = 1.57$ kΩcm^2, $U = 8.51$ V vs. SHE (top), $R_{\rm ext}A = 0.78$ kΩcm^2, $U = 8.23$ V vs. SHE (middle) and $R_{\rm ext}A = 0.69$ kΩcm^2, $U = 8.20$ V vs. SHE (bottom).

performed with a constant time average of the voltage drop across the Si|SiO_2|electrolyte-interface of

$$\overline{U_{\rm el}} := U - R_{\rm ext} A \bar{j} = 8 \text{ V vs. SHE}, \quad (1)$$

where U is the applied voltage, A the sample area and $\bar{j}$ the time average of the current density. Three time series of current j and oxide layer thickness ξ are shown in Fig.(2). When the transition between oscillatory and non-oscillatory regime is approached by gradually decreasing the external resistance, the amplitude shrinks following the square root of the distance to the critical resistance value, $R_{\rm ext,c}$, where the transition occurs. This behavior is shown in a bifurcation diagram in Fig.(3). Figure (3) does not distinguish between the two modeling frameworks, it is in fact compatible with the onset of the macroscopic oscillations due to a Hopf bifurcation and due to a Kuramoto-type synchronization of oscillating microdomains [13]. However, our measurements also make clear that it is untrue to

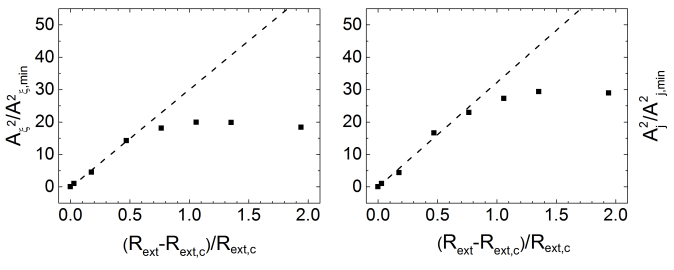

Figure 3: Squared amplitudes of the oxide layer thickness ξ (left) and the current density j (right) normalized to the lowest measured value as a function of the normalized distance in $R_{\rm ext}$ from the bifurcation point at $R_{\rm ext,c}A = 0.67$ kΩcm^2, together with linear regressions through 4 points closest to the bifurcation ($c_{\rm F} = 60$ mM, pH $= 1$). The applied voltage is set in a way that the average voltage drop across the electrode during the oscillations is identical for all measurements $\overline{U_{\rm el}} = 8$ V vs. SHE.

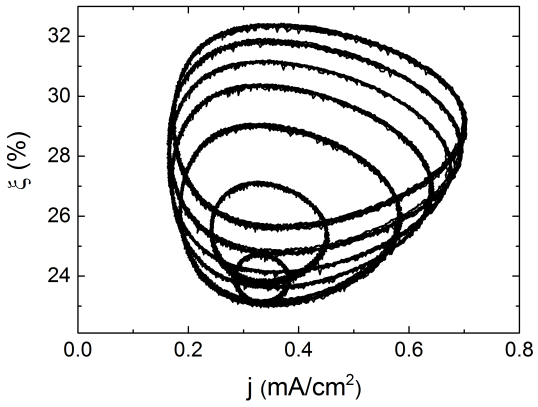

Figure 4: $j\xi$-phase space plots for the oscillatory states used for the bifurcation diagram in Fig.(3). The applied voltage is set in a way that the average voltage drop across the electrode during the oscillations, $\overline{U_{\rm el}}$ = 8 V vs. SHE, is identical for all measurements ($c_{\rm F}$ = 60 mM, pH = 1).

assume that the external resistance essentially only acts as a global coupling while it does not change the local oscillatory dynamics. This is shown in Fig.(4), where phase space portraits of oscillations for different values of $R_{\rm ext}$ but identical $\overline{U_{\rm el}}$ are shown. Clearly, the average oxide layer thickness $\overline{\xi}$ changes as a function of the external resistance, evidencing that the local oscillatory dynamics is affected by the introduction of the external resistance even when the average voltage drop across the electrode, $\overline{U_{\rm el}}$, stays constant. This in itself is again consistent with both modeling frameworks. However, since the local dynamics changes, any model developed in the local oscillator framework would have to account for this change as well since it would not cancel out via partial desynchronization of the local oscillators. The obvious question would then be whether the addition of the degree of synchronization into the model would still be necessary. The changes in the local dynamics are furthermore dependent on the specific way the transition between the globally oscillatory and the globally non-oscillatory state is approached experimentally. If $\overline{U_{\rm el}}$ is allowed to change and other central parameters such as the applied voltage U or the external resistance $R_{\rm ext}$ are kept constant instead, the time average of the oxide layer thickness $\overline{\xi}$, and thus the local dynamics, changes as well but in a different way [5, 22]. This means that in whichever way the transition to the oscillatory state was probed so far, a change in the local dynamics ensued as well. An even stronger case in point is shown in Fig.(5) where a typical oscillatory transient to a steady state upon a voltage jump from open circuit potential to U = 8.65 V vs. SHE is shown. During the oscillatory transient the ellipsometric intensity gradually drifts upwards while the oscillation amplitude decreases, the latter finally vanishing above a certain threshold thickness. This link between the upward drifting ξ and the downward trend in the oscillation amplitude clearly shows that the local dynamics changes along with the oscillation amplitude during the transient oscillations. In turn, this again corroborates a view where this change in the local dynamics is responsible for the change in the oscillation amplitude and thus part of the overall oscillation mechanism.

Our most important experimental finding in the present context is that all measurements are spatially uniform on the length scale probed, regardless of the amplitude of the stable oscillations. This is true even for the transient oscillations preceding the non-oscillatory steady state. It has already been pointed out in earlier publications from our group that the uniformity of the oscillations is always given when potentiostatic oscillations at either p-doped or highly illuminated n-doped samples are measured [5, 23]. To elucidate these finding a series of temporal evolutions of 1d cuts through the recorded data of $\xi(\vec{x})$ and electrode snapshots of $\xi(\vec{x})$ is shown in Fig.(6). The pixel dimensions in Fig.(6) are 20 μm in the x-direction and 7 μm in the y-direction. It is clear that no hint of any form of spatial variation in the oscillation period or phase is found on the spatial scale presented, irrespective of the oscillation amplitude. We attribute all deviations from a perfectly uniform behavior to noise. To justify this view, in Fig.(7) two local time series from randomly chosen points in the 1d cut shown in Fig.(6) c) are compared to the spatial average over the entire electrode for single pixels and local averages, respectively. The relatively strong noise visible in the top panel is for the most part attributable to the fact that the CCD chip used can only record 256 gray levels, leading to a resolution limit in $\xi(\vec{x})$ of ca. 0.4 % which becomes relevant at these low oscillation amplitudes. This means that the noise is a digitization error for the most part. Already a relatively small local binning of time series leads to a significant decrease of the noise as seen in the bottom panel. In both cases the spatially averaged signal represents a smoothed version of the curves and we are thus quite confident in declaring the measurements proof of a uniformity of the oscillations down to a 30×10 μm^2 scale. Note that the measurement chosen for Fig.(7) has a rather small amplitude and the degree of synchronization would thus be correspondingly small in the local oscillator framework. In addition to this, consider again the transient oscillation shown in Fig.(6) e), here the degree of synchronization should drop significantly below the level discussed so far

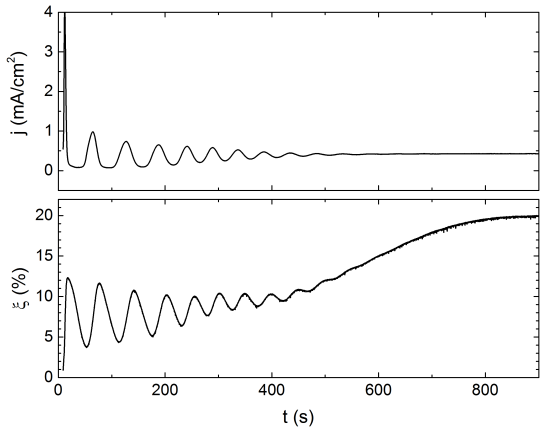

Figure 5: Oscillatory transients of current j (top) and oxide layer thickness ξ (bottom) of a non-oscillatory state initiated without an oxide layer (U = 8.65 V vs. SHE, $c_{\rm F}$ = 60 mM, pH = 1, $R_{\rm ext}A$ = 0 kΩcm^2).

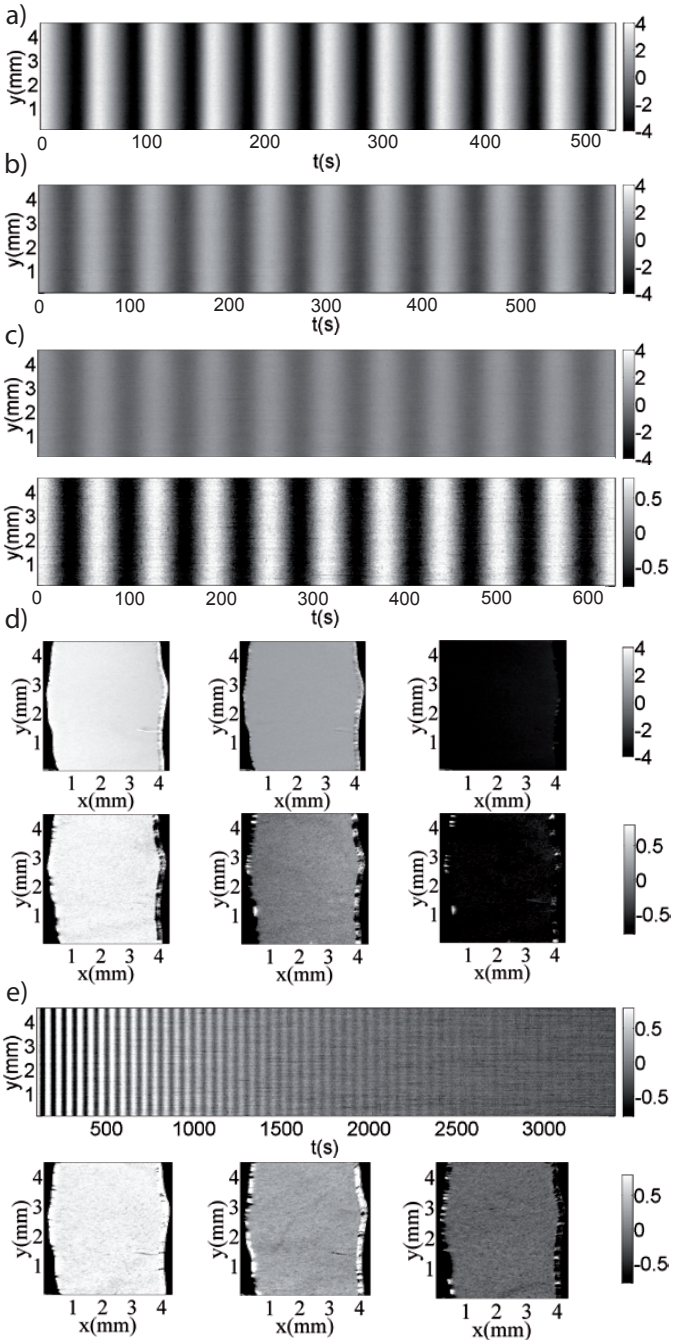

Figure 6: Plots of $\xi(\vec{x})$ for oscillations with a constant $\overline{U_{\rm el}}$ = 8 V vs. SHE in an electrolyte with $c_{\rm F}$ = 60 mM, pH = 1. Temporal evolution of a 1d cut in y-direction at x = 1.67 mm for **a)** $R_{\rm ext}A$ = 1.57 kΩcm^2, **b)** $R_{\rm ext}A$ = 0.78 kΩcm^2 and **c)** $R_{\rm ext}A$ = 0.69 kΩcm^2 (two different color scales). **d)** Electrode snapshots at three different oscillation phases, from left to right, t = 475 s, t = 489 s and t = 508 s for $R_{\rm ext}A$ = 1.57 kΩcm^2 (top) and, from left to right, t = 569 s, t = 583 s and t = 600 s for $R_{\rm ext}A$ = 0.69 kΩcm^2 (bottom). **e)** Temporal evolution of a 1d cut in y-direction and electrode snapshots at three oscillation maxima at t = 601 s (left), t = 1207 s (middle) and t = 2615 s (right) for the transient preceding a stable focus with an external resistance below the critical value ($R_{\rm ext}A$ = 0.59 kΩcm^2).

in the course of the measurement but again no hints of spatial inhomogeneities can be seen. The only way to introduce some

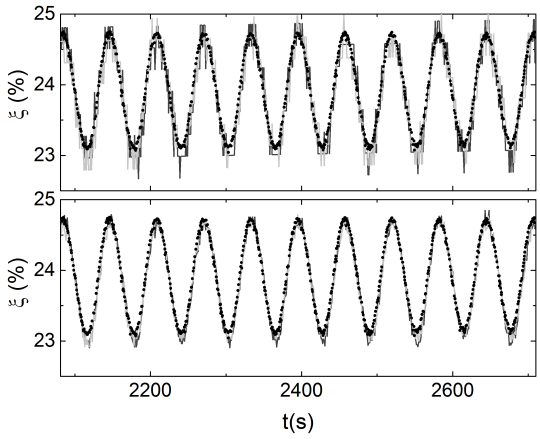

Figure 7: Local time series of $\xi(\vec{x})$ from the 1d cut in Fig.(6) c) at y = 2.14 mm (dark gray) and y = 3.21 mm (light gray) compared to the spatially averaged signal $\langle\xi\rangle$ (dots). The local time series are representing a single pixel (top) and a nearest neighbor average, i.e. a 60×21 μm^2 spot (bottom).

spatial disturbances into the system is by deliberately letting the experimental parameters vary across the electrode surface. An example of this is shown in Fig.(8), where measurements with and without magnetic stirring are compared. In the unstirred, stagnant cases, fast waves in the oxide thickness can be discerned, which are obviously caused by lateral concentration differences in some key chemical species that develops in front of the electrode. Yet, quite remarkably, a high degree of spatial coherence can be found even in the presence of the waves irrespective of the amplitude of the oscillations. Specifically, the

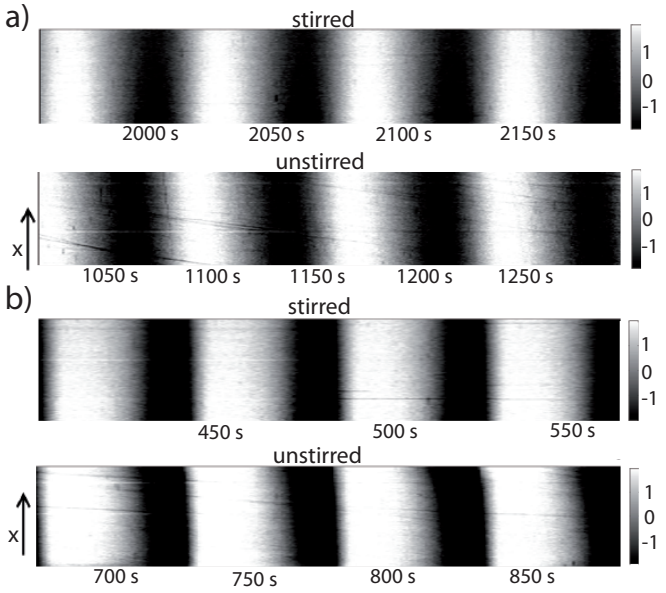

Figure 8: Comparison between 1d cuts of measurements carried out in stirred and unstirred electrolyte (U = 8.65 V vs. SHE, $c_{\rm F}$ = 50 mM, pH = 3) at $R_{\rm ext}A$ = 2.7 kΩcm^2 with a low oscillation amplitudes a) and at $R_{\rm ext}A$ = 13.5 kΩcm^2 with a high oscillation amplitudes (b). In both cases a clear spatial wave is present for the unstirred measurements.

frequencies of the individual points at the surface are identical and only the phases are shifted.

4. Discussion

In light of the experimental findings discussed so far, we now want to proceed by comparing how the two modeling frameworks stand up to the experimental evidence.

4.1. The case for the oscillatory medium approach

Our proposed framework for the modeling is that the system can be seen as a uniform oscillatory medium. This means that the oscillation mechanism is inherent to a spatially uniform oxide growth and thus fully compatible with the spatial uniformity of the oscillations presented here. We will now demonstrate that the three experimental findings from literature, which were the original motivation for the local oscillator framework, are also as easily explicable in this view as in the local oscillator model. They are thus identified as being insufficient to distinguish between the two frameworks of modeling.

The role of the external resistance is twofold since it acts not only as a global coupling between the individual points at the surface but changes the dynamics of each point in an identical manner as well. The latter is in our view of central importance and should be highly relevant if some key dynamical variables are electrical, i.e. linked to the total voltage drop across the silicon electrode U_{el}. In fact, such a connection can be made and the development of the shape of the oscillations with increasing external resistance is in good agreement with the assumption that the oscillations arise from a Hopf bifurcation [5]. In particular, for relatively low external resistances sinusoidal oscillations with an amplitude increasing with the square root of the distance in the bifurcation parameter from the bifurcation point are expected. This is exactly the behavior found in the silicon electrodissolution system as shown in Fig.(3) and the view of the external resistance as a bifurcation parameter is thus fully justified.

Moving on to the impedance spectra the observed resonances also occur when a system is in a weakly damped state close to a Hopf bifurcation, not only when it is oscillatory. This forced, weakly damped state may then inherit some features from the state at the far side of the bifurcation, a phenomenon typically referred to as the 'ghost' of the bifurcation. Specifically, in this case the occurrence of $1 : n$ and $n : 1$ resonances when forcing a stable focus would be the ghost of the Arnold tongues of the corresponding externally forced oscillatory system at the other side of the Hopf bifurcation. This effect should be very pronounced in the silicon electrodissolution system since the focus is only weakly attracting as evidenced by the relatively long transients. We did simulate impedance spectra for an example of such a stable focus in a specific system and could verify the occurrence of resonances there [24].

Lastly, the behavior of the transient anodic current observed after a potential step to a value close to the open circuit potential is fully explicable within an oscillatory medium approach as long as the transient anodic current is linked to a variable of the system. In this case this variable will vary during the oscillations but may take the time average of the oscillatory state as its constant value in the non-oscillatory state. The same can then be said for the transient anodic current.

In our view the oscillatory medium approach is the most straightforward way of modeling the system. It is based on the assumption that the oscillations are indeed spatially uniform and do not only appear so due to an insufficient spatial resolution. The focus of the modeling attempt then lies on the identification of the basic instabilities that lead to the identified bifurcation points [5]. It is very important to note that this approach is also fully consistent with the occurrence of spatial inhomogeneities on the micro scale which was often reported in literature [12, 25]. A mechanism that relies on local effects, as for example pore formation, is also permissible in this framework as long as a meaningful coarse grained, average oxide layer property can be constructed. The main difference to a local oscillator model is that the dynamics, i.e. the behavior of the system as a whole, govern the exact behavior on the microscopic level and not the other way around. For example, if pore formation played a role, the average porosity on the coarse-grained level would be given by the momentary phase and not vice versa. Finally, a very strong case in point for the oscillatory medium approach is, surprisingly, the occurrence of spatial pattern formation in the oxide layer. We have observed these patterns in many experiments for moderately illuminated n-doped samples [23, 26]. These patterns can be well understood as dynamical phenomena in an oscillatory medium under nonlinear global coupling [27]. They are spontaneous symmetry breakings which can be well understood with a generic theoretical ansatz once the system is treated as an oscillatory medium sufficiently close to a Hopf bifurcation [28].

4.2. The case against the local oscillator framework

Apart from neglecting changes in the local dynamics introduced by the external resistance as discussed in Figs.(4) and (5), the main problem with the local oscillator framework is that it has severe difficulties accounting for the spatial uniformity of spatially resolved potentiostatic measurements with p-doped or highly illuminated n-doped silicon as shown in Fig.(6) and in earlier publications from our group [5, 23]. In the local oscillator framework, the characteristic length scale of the alleged microdomains has been estimated to be of the order of ca. 100 nm [7, 29]. Is this compatible with the measured homogeneity of the oscillations down to $10 \times 30\ \mu\mathrm{m}^2$ irrespectively of the degree of synchronization? The answer strongly relies on the type and strength of any local coupling present in the system as the presence of these types of coupling would lead to the formation of local aggregates of synchronized oscillators. Such local couplings are introduced by gradients in physical or chemical quantities that are linked to either the local current or the local properties of the oxide layer. This includes concentration gradients of chemical species, such as protons, parallel to the interface, electrical fields induced by variations in the local potential drop across the interface or variations in the mechanical stress in the oxide layer. Any of these gradients leads to a flow of the underlying quantity across the microdomain boundaries

leading to a synchronization of these domains. Indeed, there is experimental proof for the presence of at least some local coupling mechanism mediated by the electrolyte in our spatially resolved measurements as shown by the comparison of stirred and unstirred electrolytes in Fig.(8). The occurrence of spatial waves is clearly visible in the unstirred cases, which means that the local composition of the electrolyte changes across the electrode surface. These waves clearly evidence the presence of diffusional coupling in the system. Since the frequency of the oscillations sensitively depends on the pH value and fluoride concentration, in the absence of a diffusional coupling of sufficient strength, it should vary in the unstirred case. However, in the experiments only the phases of the oscillations change with position, and this in a very coherent wave-like manner, their frequencies being identical everywhere. Thus, obviously the diffusional coupling is strong enough to equalize the frequencies on the entire electrode.

To estimate the effect of this diffusional coupling on the spatial distribution of the synchronized oscillators in a partially synchronized state predicted by the local oscillator framework, we make a lower estimation of how far the synchronization of neighboring domains would spread. The effective range L of this coupling then only depends on the diffusion coefficient D and the timescale τ of the phenomenon in question via

$$L = \sqrt{D \cdot \tau}. \tag{2}$$

We assume that within about a third of this range the local coupling is felt equally by all the surrounding oscillators and thus adds to the global coupling in the system. This additional term would then lead to a higher degree of synchronization in aggregates with a characteristic length scale given by the coupling range. The relevant timescale of the silicon electrodissolution system is the oscillation period of $\tau \geq 10$ s. For a diffusion coefficient of $D \approx 10^{-5}$ cm^2/s typical for small chemical species in an aqueous electrolyte even this generous estimation would lead to $L/3 \geq 30$ μm, a size well visible in our experiments. In any partially synchronized state aggregates with sizes in the order of several 10 μm would then be expected in the experiments. In addition to this, in any electrochemical system where the voltage drop across the interface plays a role for the oscillatory mechanism, a long range coupling is introduced by the lateral potential gradient in the electrode [30]. However, a change in the potential drop across the interface is probably a part of the oscillation mechanism in the silicon electrodissolution system as the occurrence of the oscillations is strongly potential dependent [5, 17]. This effect should then induce even larger aggregates. In our view the spatially resolved experimental findings presented in Figs.(6) and (8) where no aggregates in the 10 μm region or larger were found irrespective of the oscillation amplitude, i.e. the assumed degree of synchronization, thus refute the local oscillator framework.

5. Conclusion

The aim of this article was not to present a concise model of how the oscillations in the silicon electrodissolution come about but rather to clarify which type of modeling framework is sensible for the system. As shown, the often used local oscillator framework does not stand up to experimental testing. Our proposed alternative to see the system as an oscillatory medium is by no means new, quite the contrary, it is already widely used for surface reactions and electrochemical oscillations on metal electrodes [19, 31, 32]. A good example elucidating its potential and descriptive power can be found in the description of ensembles of certain yeast cells that are all individually switched at an identical bifurcation point from a non-oscillatory to an oscillatory state in a so-called 'quorum sensing' transition [33, 34]. The overall averaged behavior is quite similar to the one of the silicon electrodissolution system but even though this system is indeed built from distinct units (yeast cells), which could all potentially oscillate individually, it still acts as an oscillatory medium where the dynamics of the entire system governs the behavior of its parts and not the other way around. Further examples of drastically different systems showing similar behavior (BZ-reaction in beads) have been published in the literature [35]. The insights obtained from the cited systems from completely different fields demonstrate how inspiring concepts of nonlinear dynamics might be for an understanding of a given system. Specifically, many examples of electrochemical systems where nonlinear dynamics has proven to be crucial for the understanding have been reported in the past [36, 37]. Employing a dynamical viewpoint leads to an exchange of cause and effect in the explanation of the behavior of many nonlinear systems leading to a different kind of understanding of the system in question. It then becomes an example where a certain type of dynamics is present which can then in turn be compared to general, theoretical concepts in the field of nonlinear dynamics.

Acknowledgments

The authors acknowledge financial support from the Deutsche Forschungsgemeinschaft (Grant No. KR1189/12-1), and the cluster of excellence Nanosystems Initiative Munich (NIM).

References

References

[1] D. R. Turner. Electropolishing silicon in hydrofluoric acid solutions. *J. Electrochem. Soc.*, 105:402–408, 1958.

[2] X. G. Zhang. *Electrochemistry of silicon and its oxides*. Kluwer Academic, 2001.

[3] V. Lehmann. On the origin of electrochemical oscillations at silicon electrodes. *J. Electrochem. Soc.*, 143(4):1313–1318, 1996.

[4] J. Proost, F. Blaffart, S. Turner, and H. Idrissi. On the origin of damped electrochemical oscillations at silicon anodes (revisited). *Chem. Phys. Chem.*, 15:3116, 2014.

[5] I. Miethe and K. Krischer. Ellipsomicroscopic studies of the anodic oxidation of p-type silicon in fluoride containing electrolytes during current oscillations. *J. Electroanal. Chem.*, 666:1, 2012.

[6] J. N. Chazalviel and F. Ozanam. A theory for the resonant response of an electrochemical system: Self-oscillating domains, hidden oscillation, and ssynchronization impedance. *J. Electrochem. Soc.*, 139/9:2501, 1992.

[7] F. Ozanam, J.-N. Chazalviel, A. Radi, and M. Etman. Resonant and nonresonant behavior of the anodic dissolution of silicon in fluoride media: An impedance study. *J. Electrochem. Soc.*, 139:2491, 1992.

[8] J. Carstensen, R. Prange, G. S. Popkirov, and H. Föll. A model for current oscillations in the Si-HF system based on a quantitative analysis of current transients. *Appl. Phys. A*, 67:459, 1998.

[9] J. Grzanna, H. Jungblut, and H. J. Lewerenz. A model for electrochemical oscillations at the Si vertical bar electrolyte contact Part I. Theoretical development. *J. Electroanal. Chem.*, 486(2):181–189, 2000.

[10] J. Grzanna, H. Jungblut, and H. J. Lewerenz. A model for electrochemical oscillations at the Si vertical bar electrolyte contact Part II. Simulations and experimental results. *J. Electroanal. Chem.*, 486(2):190–203, 2000.

[11] E. Foca, J. Carstensen, and H. Föll. Modelling electrochemical current and potential oscillations at the Si electrode. *J. Electroanal. Chem.*, 603(2):175–202, 2007.

[12] F. Blaffart, Q. Van Overmeere, F. Van Wonterghem, and J. Proost. In situ monitoring of electrochemical oscillations during the transition between dense and porous anodic silica formation. *J. Electrochem. Soc.*, 161(14):H874, 2014.

[13] Y. Kuramoto. *Chemical oscillations, waves, and turbulence*. Dover Publications, Inc. (Mineola, New York), 1984.

[14] S. H. Strogatz. From Kuramoto to Crawford: exploring the onset of synchronization in populations of coupled oscillators. *Physica D*, 143:1, 2000.

[15] J. N. Chazalviel, F. Ozanam, M. Etman, F. Paolucci, L. M. Peter, and J. Stumper. The p-Si/fluoride interface in the anodic region: Damped and/or sustained oscillations. *J. Electroanal. Chem.*, 327(1-2):343–349, 1992.

[16] M. Matsumura and S. R. Morrison. Anodic Properties of n-Si and n-Ge electrodes in HF solutions under illumination and in the dark. *J. Electroanal. Chem.*, 147:157, 1983.

[17] J. N. Chazalviel. Ionic processes through the interfacial oxide in the anodic dissolution of silicon. *Electrochim. Acta*, 37:865, 1992.

[18] F. Ozanam, J.-N. Chazalviel, A. Radi, and M. Etman. Current oscillations in the anodic dissolution of silicon in fluoride electrolytes. *Ber. Bunsenges. Phys. Chem.*, 95(1):98, 1991.

[19] K. Krischer, N. Mazouz, and P. Grauel. Fronts, waves, and stationary patterns in electrochemical systems. *Angew. Chem. Int. Ed.*, 40:850, 2001.

[20] M.T.M. Koper, T.J. Schmidt, N.M. Markovic, and P.N. Ross. Potential Oscillations and S-Shaped Polarization Curve in the Continuous Electrooxidation of CO on Platinum Single-crystal Electrodes. *J. Phys. Chem. B*, 105:8381, 2001.

[21] S. Malkhandi, P.R. Bauer, A. Bonnefont, and K. Krischer. Mechanistic aspects of oscillations during CO electrooxidation on Pt in the presence of anions: Experiments and simulations. *Catalysis Today*, 202:144, 2013.

[22] K. Schönleber and K. Krischer. High-amplitude versus low-amplitude current oscillations during the anodic oxidation of p-type silicon in fluoride containing electrolytes. *Chem. Phys. Chem.*, 13:2989, 2012.

[23] K. Schönleber, C. Zensen, A. Heinrich, and K. Krischer. Pattern formation during the oscillatory photoelectrodissolution of n-type silicon: turbulence, clusters and chimeras. *New J. Phys.*, 16:063024, 2014.

[24] C. Zensen, K. Schönleber, F. Kemeth, and K. Krischer. A capacitance mediated positive differential resistance oscillator model for electrochemical systems involving a surface layer. *J. Phys. Chem. C*, 118:24407, 2014.

[25] M. Bailes, S. Böhm, L. M. Peter, D. J. Riley, and R. Greef. An electrochemical and ellipsometric study of oxide growth on silicon during anodic etching in fluoride solutions. *Electrochim. Acta*, 43 (12-13):1757, 1997.

[26] I. Miethe, V. Garcia-Morales, and K. Krischer. Irregular subharmonic cluster patterns in an autonomous photoelectrochemical oscillator. *Phys. Rev. Lett.*, 102:194101, 2009.

[27] L. Schmidt, K. Schönleber, K. Krischer, and V. Garcia-Morales. Coexistence of synchrony and incoherence in oscillatory media under nonlinear global coupling. *Chaos*, 24(1):013102, 2014.

[28] L. Schmidt and K. Krischer. Clustering as a prerequisite for chimera states in globally coupled systems. *Phys. Rev. Lett.*, 114:034101, 2015.

[29] F. Ozanam, N. Blanchard, and J.-N. Chazalviel. Microscopic, self-oscillating domains at the silicon surface during its anodic dissolution in a fluoride electrolyte. *Electrochim. Acta*, 38/12:1627, 1993.

[30] K. Krischer. *Advances in Electrochemical Science and Engineering Vol. 8*, chapter 2, pages 90–203. Wiley-VCH Verlag GmbH & Co. KGaA, 2002.

[31] G. Ertl. Oscillatory kinetics and spatio-temporal selforganization in reactions at solid surfaces. *Science*, 254:1750, 1991.

[32] J. Christoph and M. Eiswirth. Theory of electrochemical pattern formation. *Chaos*, 12:215, 2002.

[33] S. Danö, P. G. Sörensen, and F. Hynne. Sustained oscillations in living cells. *Nature*, 402:320, 1999.

[34] S. De Monte, F. d Ovidio, S. Danö, and P. G. Sörensen. Dynamical quorum sensing: Population density encoded in cellular dynamics. *Proc. Natl. Acad. Sci.*, 104(47):18377, 2007.

[35] A. F. Taylor, M. R. Tinsley, F. Wang, Z. Huang, and K. Showalter. Dynamical quorum sensing and synchronization in large populations of chemical oscillators. *Science*, 323:614, 2009.

[36] M.T.M. Koper. Non-linear phenomena in electrochemical systems. *J. Chem. Soc., Faraday Trans.*, 94(10):1369, 1998.

[37] K. Krischer. *Modern Aspects of Electrochemistry, Nr. 32*, chapter 1, page 1. Kluwer Academic/ Plenum Publisher, 1999.